Complex Activity and Short-term Memories in Reciprocally Connected Cerebral Organoids

Authors: Tatsuya Osaki[1], Yoshiho Ikeuchi[1]*

Affiliations:

[1] Institute of Industrial Science, The University of Tokyo, Meguro, Tokyo 153-8505, Japan.

*E-mail: yikeuchi@iis.u-tokyo.ac.jp

Abstract: Macroscopic axonal connections in the human brain distribute information and neuronal activity across the brain. Although this complexity previously hindered elucidation of functional connectivity mechanisms, brain organoid technologies have recently provided novel avenues to investigate human brain function by constructing small segments of the brain *in vitro*. Here, we describe the neural activity of human cerebral organoids reciprocally connected by a bundle of axons. Compared to conventional organoids, connected organoids produced significantly more intense and complex oscillatory activity. Optogenetic manipulations revealed that the connected organoids could re-play and recapitulate over time temporal patterns found in external stimuli, indicating that the connected organoids were able to form and retain temporal memories. Our findings suggest that connected organoids may serve as powerful tools for investigating the roles of macroscopic circuits in the human brain – allowing researchers to dissect cellular functions in three-dimensional *in vitro* nervous system models in unprecedented ways.

Introduction

Human induced pluripotent stem (iPS) cells have demonstrated potential for elucidating the development, function, and pathophysiology of human organs, including the brain. Recent advances in stem cell research have enabled the formation of three-dimensional tissues known as organoids, which have further unlocked the capabilities of human iPS cells. Organoid technologies have attracted increasing attention [1,2] due to their unprecedented potential for modeling human organs *in vitro*. Organoid research has advanced substantially based on accumulated knowledge on organ formation mechanisms in the fields of developmental biology and stem cells. *In vivo*-like differentiation and self-organization can be achieved in organoids by mimicking *in vivo* development with growth factors and morphogens applied at appropriate timepoints and dosages. Organoids have widespread applications, especially in neuroscience, given the difficulties of investigating human brains non-invasively. Organoids of brain regions including the cerebral cortex, thalamus, cerebellum, hippocampus, and choroid plexus have been reported [3-8], offering new platforms to investigate human brain regions *in vitro*. Although the structural and morphological characteristics of organoids highly resemble developing human brains, improving organoid functionality remains a challenge.

Recent studies have demonstrated that cerebral organoids exhibit robust oscillatory neuronal activity [9]. Cerebral organoids cultured for over 6 months gain oscillatory waves that resemble electroencephalography (EEG) activity patterns ('delta' band activity) of preterm neonatal human brains. This finding suggests that brain organoids can serve as a new model of human brain activity. Further extension of culture duration does not increase the complexity of neural activity, implying that the current approach has intrinsic limitations in the development of brain organoids. As such, additional techniques to accelerate the maturation and function of brain organoids are essential to

advance brain organoid research.

A current structural limitation of brain organoids is the lack of macroscopic connections bridging distant brain regions [10,11]. Unlike other organs in the human body, the brain is composed of functionally and structurally non-repetitive regions. Distinct brain regions are interconnected by reciprocal axonal projections that conduct action potentials to enable information processing across multiple regions, enabling higher cognitive function. The unique structural and functional features of the brain pose a major challenge for brain organoid research. Self-assembly of differentiating pluripotent stem cells precisely mimics organ development *in vivo* at the microscopic cellular level. However, organoids only model small regions of the brain unless further instructed. Interactions between adjacent brain regions have been successfully modeled by fusing organoids mimicking two distinct brain regions [12], but models of macroscopic axonal connections between distant regions, e.g. interconnected cortical areas positioned far apart, are lacking. Thus, modeling axonal connections between physically separated regions with organoids is critical to advance our understanding of the brain.

An 'organoids-on-a-chip' model of cerebral tracts has been generated by connecting two cerebral organoids via a bundle of axons that extends reciprocally in a 'handshake' manner, similar to that in developing brains [13]. In this model, a microfluidic compartment regulates the direction and assembly of growing axons, resulting in the formation of thick axon bundles that connect two cerebral organoids. In this study, we hypothesized that 'connected organoids' recapitulate the fundamental principles of macroscopic circuits and information processing. We produced axonally connected cerebral organoids from human iPS cells on a multi-electrode array and analyzed their neuronal activity. We observed highly complex activity in the connected organoids characterized by delta (0.5–4 Hz) and theta (4–8 Hz) components in relatively short-term cultures (7–8 weeks). Optogenetic inhibition of axonally transmitted neuronal activity revealed that the connections between organoids were critical for generating complex activity. The activity of the connected organoids adapted to the temporal frequency of external stimuli, and activity was sustained at an elevated frequency after stimulation was terminated. Adaptation of activity to temporal stimulation patterns required an induction delay period for the first stimulation. Further, the connected organoids regained the temporal patterns with significantly shorter delays for repeated stimulations applied within a short time, indicating that connected organoids retained short-term memory of temporal information. Our findings highlight that connected cerebral organoids as a promising tool to model macroscopic connections in functional neural circuits.

Results and Discussion

Neuronal Activity of Reciprocally Connected Cerebral Organoids in a PDMS-MEA Chip

Many brain regions are connected by reciprocally projecting axons [10,11]. To model the simplest macroscopic neural circuits, we cultured a pair of human iPS cell-derived cerebral organoids in a microfluidic culture chip (**Fig. 1A and B**). The chip (PDMS-MEA chip) consisted of a multi-electrode array (MEA) layer, polydimethylpolysiloxane (PDMS) microfluidic layer, medium reservoir ring, and lid. The PDMS layer contains two pairs of holes, each of which receive a cerebral organoid. The two holes were connected by a channel that provided spatial cues for axons to reciprocally target the organoid at the opposite end of the channel. After 4 weeks of differentiation from human iPS cells (**Fig. 1C and D**), cerebral organoids were introduced into the holes of the PDMS-MEA chip. The two cerebral organoids connected through a thick axonal bundle in the chip within 6 weeks (2 weeks in the chip, **Fig. 1E and Fig. S1**). The thickness of the

axonal bundle was approximately 75 μm at 6 weeks and 120 μm at 8 weeks (**Fig. 1F**). vGlut1-positive excitatory neurons and GAD67-positive inhibitory neurons comprised approximately 70% and 5–10% of cells in the organoids, respectively (**Fig. 1G**). Subcortical layer structures were observed in the connected organoids (**Fig. 1H**). These results indicate that the organoids mimicked developmental brain processes as they formed reciprocal axonal connections.

Electrodes equipped under the two organoids captured neuronal activity (**Fig. 1B, I**). Action potential spikes and local field potentials (LFPs) were extracted by a high-frequency filter and low-frequency filter, respectively. At 5 weeks (1 week of culture in a chip), neuronal activity could be detected from the two cerebral organoids (**Fig. 1J**). At this stage, the activity of the two cerebral organoids was not synchronized, which was consistent with the paucity of axonal connections between the organoids at this timepoint. At 5.5–6 weeks (1.5–2 week of culture in a chip), synchronized burst-like activity was observed (**Fig. 1K**). The upsurge and synchronization of this activity coincided with the physical connectivity of the organoids via an axonal bundle. Neural activity became more synchronized, and more frequent burst-like activity was observed over time (**Fig. 1L and M**). Notably, a small temporal shift between signals from the connected organoids was observed (**Fig. 1O and N**), suggesting that spontaneous neural activity was initiated in an organoid and propagated to the other organoid through the axonal bundle. The two organoids alternated in leading signal propagation, indicating that the connections were functionally bidirectional.

Complex Neuronal Activity induced by Axonal Connections Between Cerebral Organoids

At 6 weeks (2 week of culture in a chip), slow LFP signals that were absent prior to the establishment of axonal connections were observed in the connected organoids (**Fig. 2A**). Clustered action potentials of multiple neurons produce low-frequency LFP patterns in a coordinated manner [14]. After another week of culture in a chip (7 weeks in total), the LFP patterns of the connected organoids became significantly more complex, and intense activity in the delta frequency band (0.5–4 Hz) emerged (**Fig. 2A and B**). The intense and complex activity of the connected organoids was unexpected at this relatively early stage, considering previous reports indicating that cerebral organoids exhibit delta band activity after being cultured for a few months [9]. We thus compared the neural activity of our 'connected' organoids with conventional cerebral organoids ('single' organoids). Since the connected organoids contained approximately double the number of cells, we also assessed the activity of tissues generated by directly fusing two cerebral organoids ('fused' organoids) as an additional control (**Fig. 2C and Fig. S2**). After culturing for 6 weeks, oscillatory activity was detected from all of the organoids (**Fig. 2C**). The burst-like activity was observed more often in the fused organoids than in the single organoids, suggesting that the total number of neurons in organoids influences neural activity. Notably, the connected organoids exhibited significantly more frequent burst-like activity when compared to the single or fused organoids, although the numbers of neurons in the fused and connected organoids were comparable (**Fig. 2D**). These findings suggested that axonal connections between organoids strongly enhanced neural activity in cerebral organoids.

The signal propagation velocity between the fused organoids was significantly less than that within a single organoid (**Fig. S2**), whereas the signal propagation velocity between the connected organoids was faster than that within a single organoid. The lag of signal propagation between organoids was significantly higher in the fused organoids than in the connected organoids. The axonal length did not alter the velocity of signal propagation (**Fig. S3**), indicating that the architecture of synaptic connections within the tissues determined the signal propagation velocity.

These results suggested that axonal connections between organoids served as a signal 'highway' between connected organoids and facilitated neuronal activity.

The connected organoids exhibited significantly richer activity in the delta frequency band (0.5–4 Hz) when compared to the single and fused organoids (**Fig. 2E**). To quantify the temporal complexity of the activity in a different way, we assessed the periodicity of burst-like patterns of the organoids. The coefficient of variance (CV) of burst-like events was significantly higher in the connected organoids than in the single and fused organoids (**Fig. 2F**), indicating that burst-like events occurred significantly less periodically and more intricately in the connected organoids than in the single or fused organoids. The CV increased consistently over 9 weeks of culture in the connected organoids but did not change significantly in the single organoids and fused organoids during this culture period. The fused organoids exhibited more frequent burst activity than the single organoids in consistent with their size (**Fig. 2G**), presumably due to increased total cell numbers and synapses within the tissues. Strikingly, the connected organoids exhibited burst-like activity in higher frequency than the single or fused organoids regardless of their size. These results suggested that the connected organoids comprised more complex neural circuits than the single or fused organoids, indicating that the reciprocal connections induced complex activity in the cerebral organoids.

Optogenetic Inhibition of Axon Bundles Between Connected Organoids

To test if the axonal connections critically generate the complex activity of the connected organoids, we inhibited activity transmitted through the axon bundle between the organoids. Physically severing the axonal bundle between organoids disrupted the burst-like events and LFP patterns in the delta band, highlighting the importance of macroscopic connections for generating complex neuronal oscillatory activity patterns in organoids (**Fig. S4**). To further assess the role of the axonal connections between organoids, we modified the microfluidic chip to perform optogenetic inhibition of the axonal bundle between the organoids (**Fig. 2H and Fig. S5**). ArchT was expressed in the organoids mediated by adeno-associated virus (AAV). With an optic fiber and PDMS lens, the light was used to suppress only the axon bundle in the microchannel. Illumination of the axon bundle with orange light (20 ms, 20 Hz for 5 min) robustly suppressed neuronal activity in the connected organoids, resulting in loss of high-amplitude burst-like events and low-frequency delta-LFP patterns under light illumination (**Fig. 2I**), suggesting that action potentials traveling through the axonal bundle induced burst-like activity in the connected organoids. Upon cessation of illumination, the burst-like activity and delta-LFP patterns immediately recovered. These light-induced responses were repeatedly observed after light exposure. The frequency of spontaneous burst-like events did not change after light exposure, suggesting that internal circuit properties intrinsically determined the frequency of spontaneous burst-like activity. Notably, the coherence and synchronicity of signals from the two connected organoids were significantly lost during light exposure (**Fig. 2J and K**). Indeed, optogenetic disconnection of the two organoids resulted in significant suppression of the overall intensity of neural activity, potentially mimicking surgical treatments for refractory epilepsy patients [15,16]. While burst-like events disappeared upon optogenetic inhibition of inter-organoid axons, the number of observed action potentials were increased (**Fig. 2L and M**). This demonstrated that inter-organoid axons contributed to burst-like activity by temporally orchestrating and aggregating activity of individual neurons within the two connected organoids. These results indicated that activity transmitted via the inter-organoid axon bundle underpinned complex neuronal activity in the connected organoids, supporting the importance of macroscopic connections in the brain.

Phase-Amplitude Coupling in Connected Organoids

Extension of the culture period over 8 weeks resulted in a further increase in LFP frequency and action potential spikes of the connected organoids (**Fig. S6**). The complexity of the signals also increased and exhibited rich theta band activity (**Fig. 3A**). The representative plot depicts a strong correlation of gamma activity with delta and theta activity. To examine the relationship between low-frequency activity and the amplitude of high-frequency spikes, phase-amplitude coupling (PAC) was calculated. PAC is an established method to assess the relationship between complex EEG recordings in distinct frequency bands (17, 18). Within the burst-like oscillatory activity, LFP waves in delta and theta bands emerged in a coordinated manner with synchronized bursts of activity in the gamma band (**Fig. 3A and B**). Delta-gamma PAC modulation of the connected organoids increased with culture time, followed by an increase in theta-gamma PAC modulation (**Fig. 3C**). Both delta-gamma and theta-gamma modulations in the connected organoids were significantly higher than those of the single or fused organoids (**Fig. 3D**). Examination of each interconnected organoid revealed that delta-gamma PAC and theta-gamma PAC exhibited high modulation (intra-organoid PAC). PAC between the organoids connected by the axon bundle (inter-organoid PAC) of both delta-gamma and theta-gamma modulations was higher than the intra-organoid PAC, indicating rich communication between the two organoids in delta and theta bands (**Fig. 3E**). The correlated activity between the two organoids was validated using calcium imaging methods (**Fig. S7**).

Next, we examined the neuronal avalanches of signals recorded from the connected organoids (**Fig. 3F**). Temporally proximal signals across the electrodes were grouped and quantified as neuronal avalanches. Power law exponents of neuronal avalanches are considered to be a scale-free index of network critical dynamics (19, 20). Avalanche size distributions increased over the course of culturing the connected organoids. At 5 weeks, the connected organoids exhibited an exponent of $\alpha = -2.8$ (**Fig. 3G**). As they connected via axons in the channel, the exponent increased to -2.1. At 8.5 weeks, the exponent became $\alpha = -1.6$, which approximated the theoretical exponent of $-3/2$ in the critical branching process (19, 20). We examined the observed frequency of neuronal avalanches by pattern recognition using the hidden Markov model, which revealed that patterns of action potentials increased during the culture of the organoids on the chip (**Fig. 3H**).

Dynamic Synaptic Balance Underlying the Complex Activity of Connected Organoids

To investigate the balance of synaptic receptors underlying complex activity of the connected organoids, the connected organoids were treated with antagonists for the major synaptic channels; namely, NMDA, AMPA, and GABA, with CNQX, APV, and bicuculline, respectively. No changes in the speed of signal propagation were observed (**Fig. S8**). However, the compounds affected neuronal activity observed as action potential spikes and burst-like events (**Fig. 3I-K**). As expected, CNQX and APV decreased neuronal activity, delta-gamma PAC, and theta-gamma PAC in the connected organoids (**Fig. 3L**), suggesting that excitatory synaptic transmission played a critical role in driving complex activity in the connected organoids. Spiking activity was significantly increased, whereas the number of burst-like events remained unchanged following bicuculine treatment. Burst-like events became weaker (**Fig. 3K**) following bicuculine treatment, suggesting that inhibitory synapses were critical for generating oscillatory activity in the connected organoids.

Next, we tested clinical compounds that modulate synaptic properties. Treatment with the positive GABA receptor modulators, baclofen and diazepam, decreased the number of spikes, in

accordance with the opposing effects of bicuculine. Treatment with clozapine mildly decreased neuronal activity but did not alter PAC properties. Treatment with buprenorphine specifically decreased theta-gamma PAC, indicating that buprenorphine affected the coordination of activity in different frequency bands in the connected organoids. These results highlight the potential of using connected organoids to test compounds for complex activity.

Optogenetic Stimulation-Induced Memory Formation in Connected Organoids

We characterized the evoked responses of the connected organoids using optogenetic stimulation. After expressing channelrhodopsin in the connected organoids, we stimulated the axons with pacing illumination (470 nm) at 0.5 Hz for 5 min, 1.0 Hz for 5 min, followed by 1.5 Hz for 5 min (**Fig. 4A**). The stimulation increased burst-like events in accordance with the temporal patterns of stimulation. After cessation of stimulation, the frequency of burst-like events was sustained at a high level for more than 10 min and subsequently returned to the pre-stimulation frequency (**Fig. 4B, C**). This sustained echo-like activity indicated that the temporal activity patterns of the connected organoids could be modulated by external stimulation and maintained the temporal information of stimuli, highlighting the capability of the connected organoids to retain temporal information as a primitive form of memory. Notably, the induction of burst-like events occurred with a delay after commencing the stimulation (**Fig. 4C**), suggesting that multiple stimulations were necessary for modulating the connected organoids. During the delay, the neuronal avalanches extended as the connected organoids were periodically stimulated (**Fig. 4D**), suggesting that the neurons in the connected organoids slowly adapted to the stimuli and established functional subcircuits before the connected organoids apparently followed the temporal patterns of external stimulation.

Next, we examined 'memory rehearsal' of the connected organoids with periodic optogenetic stimulation. Repeated activation of neurons ('rehearsal') is known to maintain short-term memory in the human brain. Repeated stimulation resulted in echo-like activity after cessation of the stimulation (**Fig. 4E and F**), while the sustained activity was not observed with weak stimulation. Notably, the lag before adapting to the external stimuli became significantly shorter in the second or third attempt when compared to the first stimulation (**Fig. 4G**). This indicated that the connected organoids were able to store memory of external stimulation in the first stimulation and regain this temporal pattern by repeated stimulation.

Memory formation and consolidation are regulated by synaptic plasticity through diverse molecular programs, including calcium-dependent signaling pathways and local protein synthesis. To probe the mechanisms underlying memory formation in connected organoids, we treated the organoids with K252a, which is an inhibitor of CaM kinase II, and anisomycin, which is an inhibitor of protein synthesis, during the memory formation experiment (**Fig. 4H**). The connected organoids responded to optical stimulation, and echo-like sustained activity after stimulation was observed with the drug treatment. The sustained period of post-stimulation echo-like activity decreased in the presence of K252a after the second and third stimulation (**Fig. 4I**). Anisomycin treatment resulted in a slight decrease in echo-like activity only after the third stimulation. K252a treatment inhibited the shortening of the lag after starting the stimulation until the response of the connected organoids compared to the control after the second stimulation (**Fig. 4J**). These results indicated that calcium-dependent signaling pathways underpin the memory formation observed in our experiments – a mechanism resembling short-term memory formation in the brain.

Neuronal avalanches became also smaller with K252a treatment (**Fig. 4K**). During light

exposure, the number of hidden patterns in neuronal avalanches decreased over the light-off period (**Fig. 4L and M**). Notably, the number of hidden patterns gradually increased as stimulations were repeated. Anisomycin treatment prevented the extension of hidden patterns for neuronal avalanches during the light-off period, suggesting that mechanisms for long-term memory formation were activated in the connected organoids.

To examine the underlying variability and complexity of the activity of the connected organoids, Higuchi's fractal dimension was calculated. Fractal dimension (FD) is utilized as an indicator of the complexity of EEG signals [17]. In the control, FD increased after stopping the light stimulation in the first stimulation, and the elevated FD was preserved regardless of light exposure (**Fig. 4N and O**). In the presence of K252a, FD did not increase in the first attempt, but FD increased after light stimulation in the second attempt and was preserved in the third attempt, indicating that K252a treatment perturbed memory formation through complex network activity. In contrast, FD was not altered in all attempts in the presence of anisomycin, suggesting that protein synthesis was involved in network activity dynamics even in response to stimuli that induced short-term modulations.

To assess temporal neuronal activity within burst-like activity, evoked activity was sorted and aligned (**Fig. 5A**). Closer examination revealed that optogenetic stimulations triggered multiple waves of neuronal activity within the evoked burst-like events. The latency of the burst-like events decreased with repeated rehearsal stimulations in the control (**Fig. 5B**) Such decrease in activity was observed with anisomycin treatment, but not in the presence of K252a. To dissect the evoked responses in more detail, the evoked burst probability histogram was calculated by kernel density estimation (**Fig. 5C and D**), which revealed that the first rise of the peak became earlier with repeated stimulations. Further, the stimulation triggered secondary and tertiary waves of activity more than 200 ms after the primary response, which intensified after repeated stimulation (**Fig. 5C and D**). Secondary waves were also observed with K252a or anisomycin treatment. Notably, two organoids interconnected via an axon bundle often responded to light exposure with different kinetics. (**Fig. 5E**). The secondary and tertiary waves of the evoked burst responses can be alternatingly observed in the two connected organoids (**Fig. 5E**). These results suggested that the activity in the connected organoids was generated by a complex ensemble of activity in the two organoids. To quantify the divergence of the evoked activity, we evaluated the entropy of waveforms of the burst-like events (**Fig. 5F**). Repeated stimulation increased the entropy of the evoked burst-like events; this effect was inhibited by K252a treatment. This suggested that stimulation triggered complex activity in the control connected organoids, but K252a treatment prevented the increase in entropy of the burst-like events which underpinned the short-term memory formation defects induced by K252a treatment in the connected organoids.

In conclusion, we demonstrate that connected cerebral organoids generate spontaneous high-frequency oscillations and are capable of memory formation. This system may facilitate elucidation of human brain development and memory from both physiological and pathological perspectives. To our knowledge, we provide the first evidence that cerebral organoids have primitive memory processing capability. Currently, connected organoids are only able to recapitulate the primary response in memory processing compared to the human brain. Further developments such as connecting different regions of brain organoids and/or connecting more than two organoids via axonal bundles will forge novel avenues for understanding the human brain. These would allow us not only to utilize the tissue model in biology, but also to gain clues to develop novel algorithms in information processing.

Materials and Methods

Institutional Approvals and Ethics

The use of human iPSCs was approved by the institute. All methods related to iPS cell handling were performed in accordance with approved guidelines.

Experimental Design

Human iPS Cells

Human iPS cells were obtained from the Riken Cell Bank (409B2, HPS0076). Cells were maintained on ESC-qualified matrigel-coated 6-well plates in mTeSR plus medium (STEMCELL Technologies) with 10 μM Y-23632 (only initial 24 hours, Wako) and subcultured every 5–7 days using ReLeSR (STEMCELL Technologies).

Statistical Analysis

The reported values correspond to the means of a minimum of three independent experiments. Data are presented as means ± SD. Comparisons were performed using a one-way analysis of variance (ANOVA) with post-hoc pairwise comparisons using the Tukey-Kramer method. Statistical tests were performed using GraphPad Prism.

Reference

1 Eiraku, M. *et al.* Self-Organized Formation of Polarized Cortical Tissues from ESCs and Its Active Manipulation by Extrinsic Signals. *Cell Stem Cell* **3**, 519-532, doi:https://doi.org/10.1016/j.stem.2008.09.002 (2008).

2 Lancaster, M. A. *et al.* Cerebral organoids model human brain development and microcephaly. *Nature* **501**, 373-379, doi:10.1038/nature12517 (2013).

3 Del Dosso, A., Urenda, J.-P., Nguyen, T. & Quadrato, G. Upgrading the Physiological Relevance of Human Brain Organoids. *Neuron* **107**, 1014-1028, doi:https://doi.org/10.1016/j.neuron.2020.08.029 (2020).

4 Xiang, Y. *et al.* Fusion of Regionally Specified hPSC-Derived Organoids Models Human Brain Development and Interneuron Migration. *Cell Stem Cell* **21**, 383-398.e387, doi:https://doi.org/10.1016/j.stem.2017.07.007 (2017).

5 Sakaguchi, H. *et al.* Generation of functional hippocampal neurons from self-organizing human embryonic stem cell-derived dorsomedial telencephalic tissue. *Nature Communications* **6**, 8896, doi:10.1038/ncomms9896 (2015).

6 Muguruma, K., Nishiyama, A., Kawakami, H., Hashimoto, K. & Sasai, Y. Self-Organization of Polarized Cerebellar Tissue in 3D Culture of Human Pluripotent Stem Cells. *Cell Reports* **10**, 537-550, doi:https://doi.org/10.1016/j.celrep.2014.12.051 (2015).

7 Xiang, Y. *et al.* hESC-Derived Thalamic Organoids Form Reciprocal Projections When Fused with Cortical Organoids. *Cell Stem Cell* **24**, 487-497.e487, doi:https://doi.org/10.1016/j.stem.2018.12.015 (2019).

8 Pellegrini, L. *et al.* Human CNS barrier-forming organoids with cerebrospinal fluid production. *Science* **369**, eaaz5626, doi:10.1126/science.aaz5626 (2020).

9 Trujillo, C. A. *et al.* Complex Oscillatory Waves Emerging from Cortical Organoids Model Early Human Brain Network Development. *Cell Stem Cell* **25**, 558-569.e557, doi:https://doi.org/10.1016/j.stem.2019.08.002 (2019).
10 Zingg, B. *et al.* Neural networks of the mouse neocortex. *Cell* **156**, 1096-1111, doi:10.1016/j.cell.2014.02.023 (2014).
11 Swanson, L. W., Hahn, J. D. & Sporns, O. Organizing principles for the cerebral cortex network of commissural and association connections. *Proc Natl Acad Sci U S A* **114**, E9692-E9701, doi:10.1073/pnas.1712928114 (2017).
12 Bagley, J. A., Reumann, D., Bian, S., Lévi-Strauss, J. & Knoblich, J. A. Fused cerebral organoids model interactions between brain regions. *Nature Methods* **14**, 743-751, doi:10.1038/nmeth.4304 (2017).
13 Kirihara, T. *et al.* A Human Induced Pluripotent Stem Cell-Derived Tissue Model of a Cerebral Tract Connecting Two Cortical Regions. *iScience* **14**, 301-311, doi:10.1016/j.isci.2019.03.012 (2019).
14 Buzsáki, G., Anastassiou, C. A. & Koch, C. The origin of extracellular fields and currents--EEG, ECoG, LFP and spikes. *Nat Rev Neurosci* **13**, 407-420, doi:10.1038/nrn3241 (2012).
15 Spencer, S. S. *et al.* Corpus callosotomy for epilepsy. *I. Seizure effects* **38**, 19-19, doi:10.1212/wnl.38.1.19 (1988).
16 Paul, L. K. *et al.* Agenesis of the corpus callosum: genetic, developmental and functional aspects of connectivity. *Nature Reviews Neuroscience* **8**, 287-299, doi:10.1038/nrn2107 (2007).
17 Varley, T. F. *et al.* Fractal dimension of cortical functional connectivity networks & severity of disorders of consciousness. *PLOS ONE* **15**, e0223812, doi:10.1371/journal.pone.0223812 (2020).

Acknowledgments:

We thank Drs. Yoji Hirano, Shoichiro Nakanishi, Yusuke Hirabayashi, Yoshito Masamizu, Parizad Billimoria, Kazuyuki Aihara, and the Ikeuchi lab members for discussion and critical comments. We thank Drs. Teruo Fujii, Soo Hyeon Kim, and Marie Shinohara for generously providing support on micro fabrications. **Funding:** This work was supported in part by the Japan Society for the Promotion of Science (JSPS) with a Grant in Aid for Early-Career Scientists (20K20178), AMED-P-CREATE (G02-53), and Takeda Science Foundation (T.O.), the Ministry of Education, Culture, Sports, Science and Technology (MEXT), a Grant-in-Aid for Scientific Research on Innovative Areas in the ‘‘Nascent Chain Biology’’ category (17H05661), the Japan Society for the Promotion of Science (JSPS) with a Grant-in-Aid for a Challenging Research (Pioneering) (20K20643), and the Grant-in-Aid for Transformative Research Areas (B) (20H05786), AMED-CREST, AMED (JP20gm1410001), Institute for AI and Beyond, and Casio Science Promotion Foundation (Y.I.).; **Author contributions:** T.O. and Y.I. conceived and designed the experiments. T.O. performed the experiments and data analyses. T.O. and Y.I. wrote the manuscript; **Competing interests**: Authors declare no competing interests; **Data and materials availability**: All data used to reach the conclusions in this paper are presented in the paper and Supplementary Materials. Additional data related to this paper may be requested from the authors.

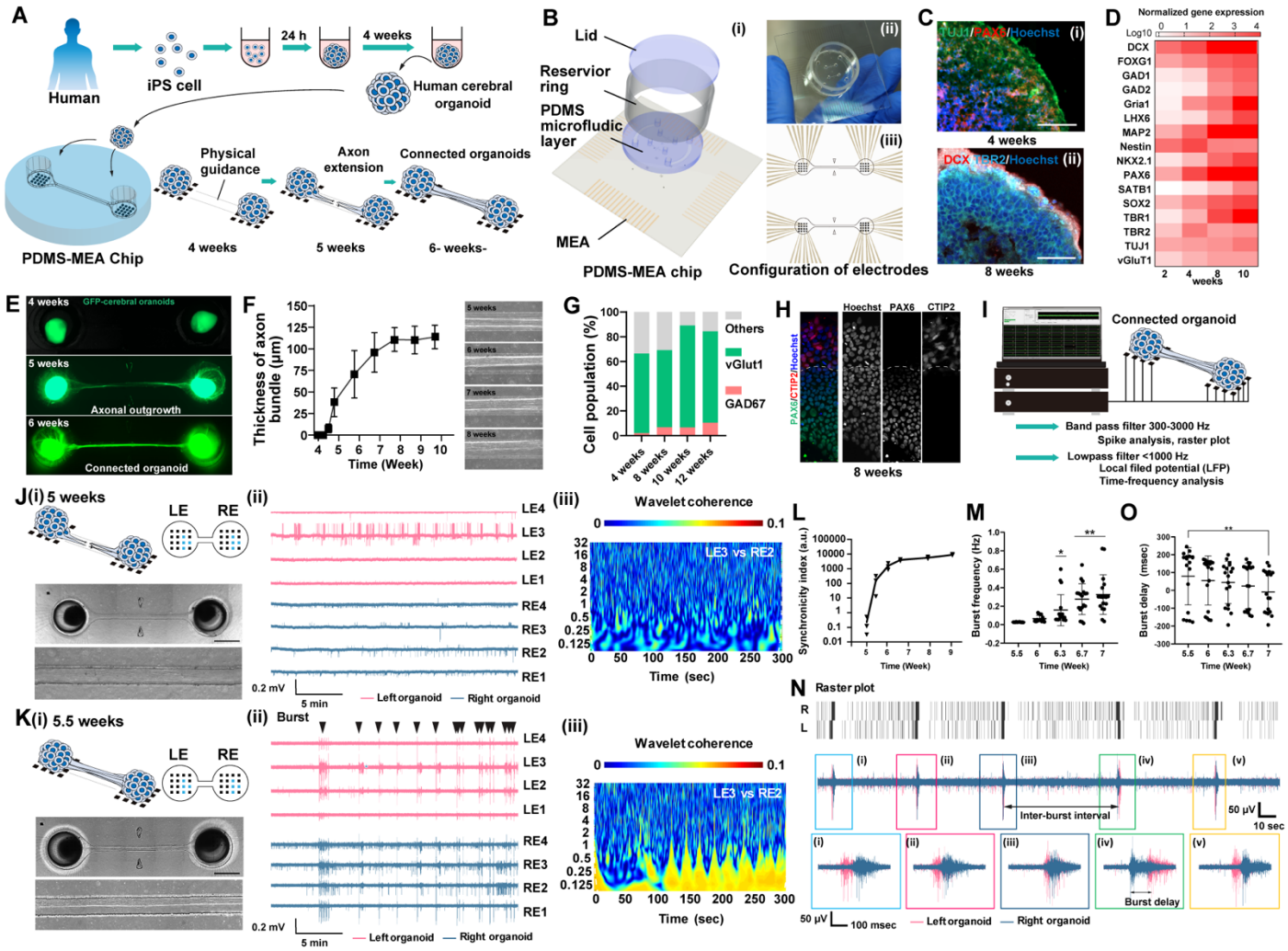

Fig. 1. Formation and characterization of the connected organoids in a PDMS-MEA chip

(A) Schematic drawings of connected cerebral organoids in a PDMS-MEA chip. Two cerebral organoids were introduced into two chambers bridged by a microchannel in a chip. (B) A PDMS-MEA chip consisted of an MEA probe, patterned PDMS, glass reservoir ring, and PDMS lid (i, ii). Sixteen electrodes (four-by-four array) were located underneath each organoid (iii). (C) Representative internal structures at 4 and 8 weeks. Scale bar: 150μm. (D) Gene expression profiles in the cerebral organoids from 2 to 10 weeks of culture. (E) Axons projected from one organoid to another in 5 weeks, and thick axonal bundles were formed by 6 weeks. (F) Time-course of axon bundle thickness. n = 6. (G) The ratio of excitatory neurons and inhibitory neurons in the organoids. n = 3. (H) Immunohistochemical analyses revealed layer structures within the connected organoids after 8 weeks of culture. Immunoreactivity against PAX6 and CTIP2 indicates the proliferative layer and cortical sublayer, respectively. (I) Recording of neuronal activity from the connected organoids in the chip. Raw analog signals from electrodes were amplified and converted to digital signals (16 bit) at a 20 kHz sampling rate. Then, the signal was processed with a 300–3,000 Hz band pass filter or a 1,000 Hz low pass filter for spike analysis and local field potential (LFP) analysis, respectively. (J) Representative images of connected organoids at 5 weeks of culture (i). Scale bar: 1 mm. Filtered signals from four representative electrodes

under each organoid (ii). Wavelet coherence between signals from an electrode under an organoid and another electrode under the other connected organoid (iii). (K) Representative images of the connected organoid at 5.5 weeks of culture (i). Scale bar: 1 mm. Synchronized burst-like activity associated with dense spikes was observed from multiple electrodes (ii). Wavelet coherence indicated a strong correlation between the two connected organoids (iii). (N) Synchronicity of activity in the two connected organoids increased during the culture period. (M) Burst frequency increased significantly with culture time. (N) Magnified view of plot of neuronal activity of the two connected organoids. Synchronized burst activity was observed with delay. (O) Burst delay at different culture periods. n = 20. *$p<0.05$, **$p<0.01$; one-way ANOVA. Error bars indicate SD.

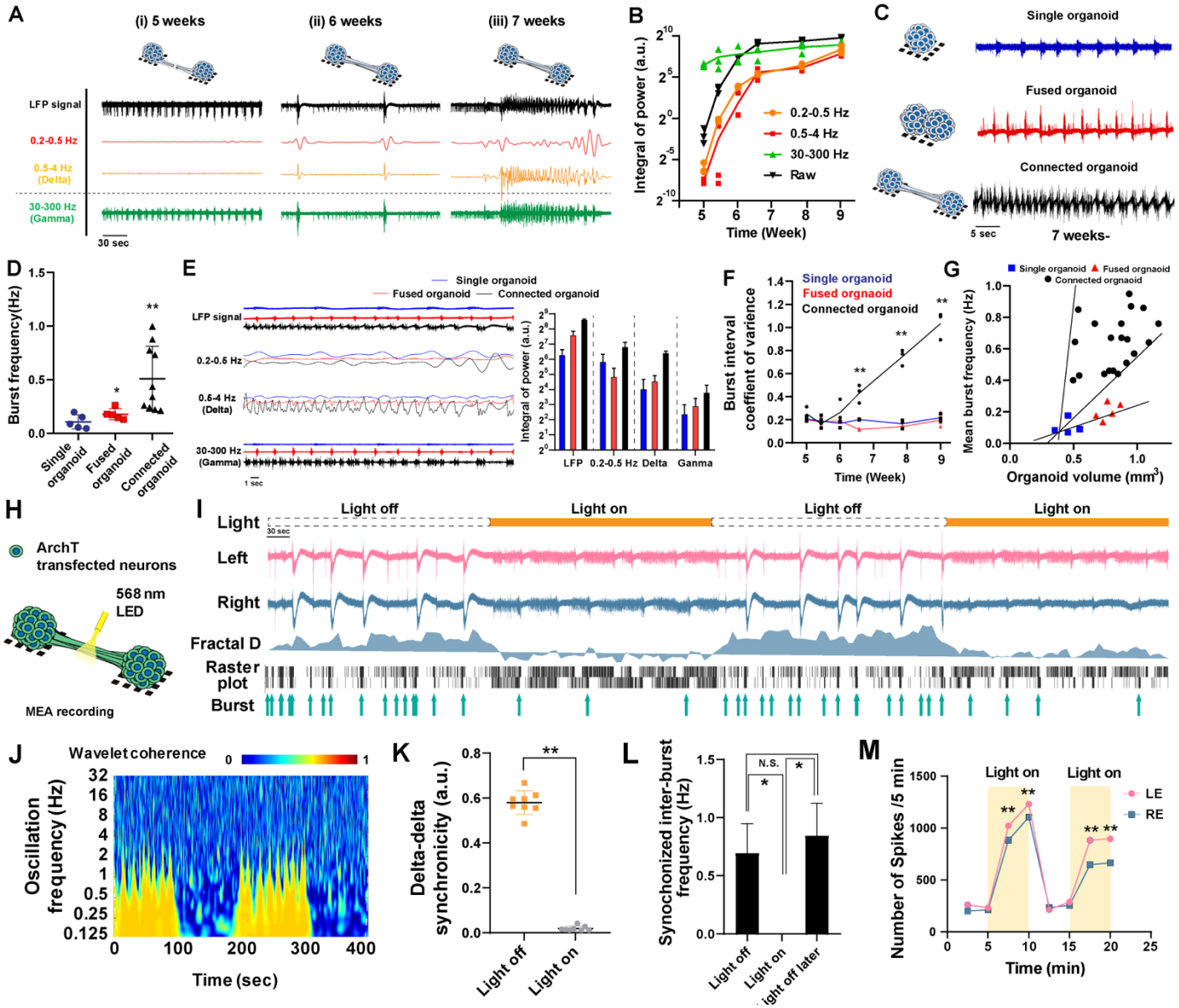

Fig. 2. Reciprocal connections through bundled axons generate complex neuronal activity

(A) LFP signals were extracted from the 0.2–0.5 Hz, 0.5–4 Hz (delta), and 30–300 Hz (gamma) bands by inverse continuous wavelet transformation. At 8 weeks, the connected organoids generated slow wave oscillations in the 0.5–4 Hz (delta) band. (B) Integral of power in wevelentgh-bands. (C) Representative neuronal activity of the connected, single, and fused organoids. (D) Burst frequency of the organoids. n = 10. (E) Inverse continuous wavelet transformation in the 0.2–0.5 Hz, 0.5–4 Hz (delta), and 30–300 Hz (gamma) bands. Delta band oscillations were observed in the connected organoids but not in the single and fused organoids. (F) Inter-event interval coefficient of variance among three types of organoids. (G) Relationship between organoid volume and mean inter-burst frequency. (H) Optogenetic set up for inhibiting the synaptic interactions between the two connected organoids via the inter-organoid axonal bundle. (I) LFP and raster plot of the two connected organoids with or without light illumination. (J) Wavelet coherence revealed that slow wave oscillations disappeared during light illumination, indicating

the absence of inter-organoid correlated activity during light exposure. n = 8. (K) Inter-organoid synchronicity measured by delta phase-delta phase coupling exhibited a significant decrease during light illumination. (L) Light-induced inhibition of the axonal bundle suppressed overall burst-like events. (M) Total number of action potential spikes in 5 min was quantified. Light exposure significantly increased isolated spikes. *$p<0.05$, **$p<0.01$; one-way ANOVA. Error bars indicate SD.

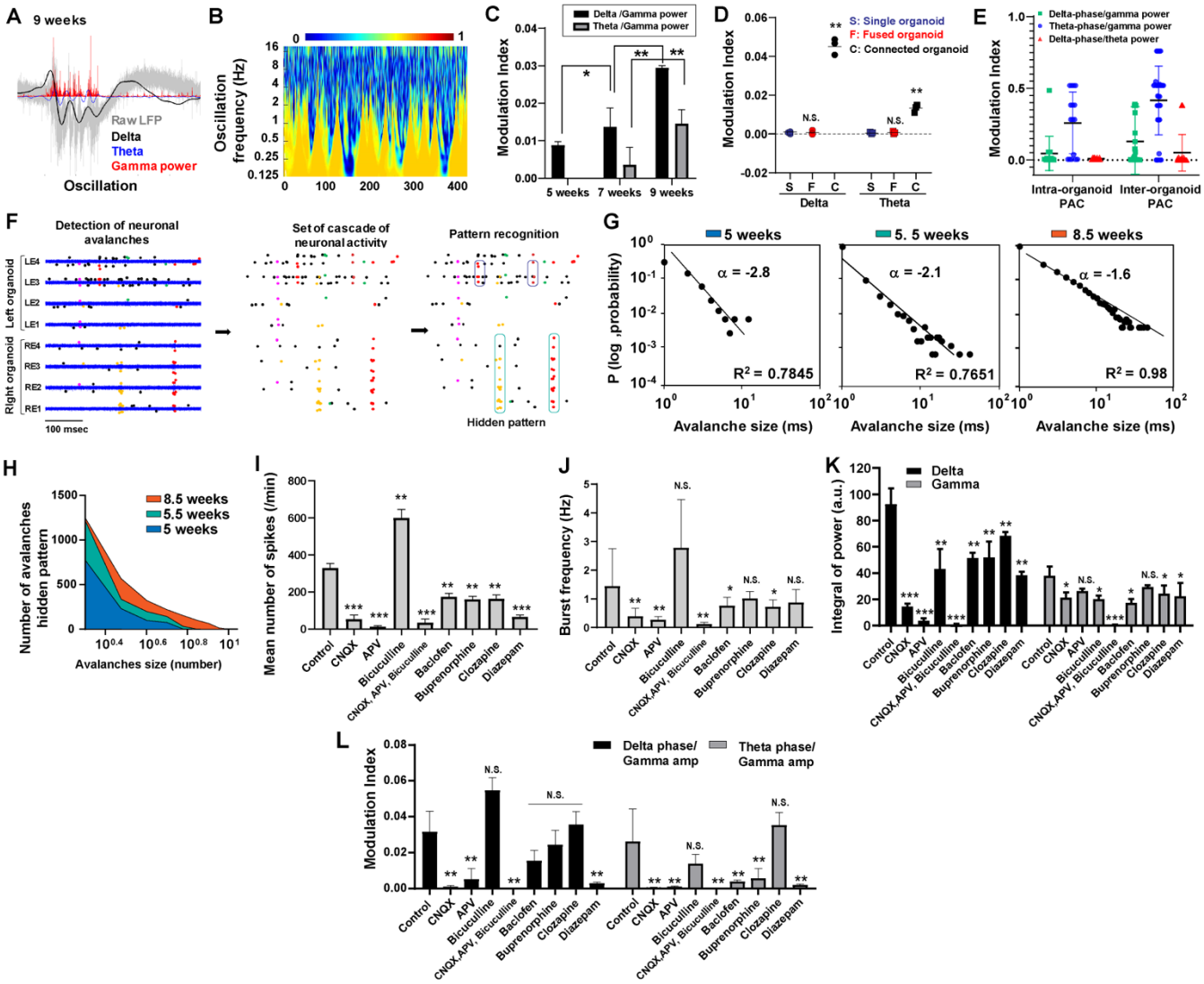

Fig. 3. Theta-band oscillation, phase-amplitude coupling, and neuronal avalanches indicate complex activity in the connected organoids

(A) Raw LFP plot from four electrodes of each of the connected organoids at 9 weeks. (B) Wavelet coherence between the two organoids exhibited synchronous activity in the theta band frequency. (C) Modulation index of phase-amplitude coupling in delta-phase/gamma-power and theta-phase/gamma-power of the connected organoids cultured for 5, 7, and 9 weeks. (D) Delta-phase/gamma-power and theta-phase/gamma-power PAC modulation index of single, fused, and connected organoids. (E) Intra- or inter-organoid PAC modulation index in the connected organoids. (F) Schematic illustration of analyses of neuronal avalanches including the extraction of neuronal avalanche cascades and hidden pattern recognition by Markov model. Neuronal avalanches were calculated from 8 electrodes. The cascade of single spikes was characterized at 3 msec scale size. (G) The log plot of neuronal avalanche size and probability at 5, 5.5, and 8.5 weeks of culture. (H) The number of hidden patterns in neuronal avalanches at 5, 5.5, and 8.5 weeks. (I, J, K, L) Comparison of activity patterns of the connected organoids upon treatment with neuromodulator compounds. Mean number of spikes (I), burst frequency (J), power integral in

delta band (K), and PAC modulation index (L) were assessed. *$p<0.05$, **$p<0.01$; one-way ANOVA. Error bars indicate SD.

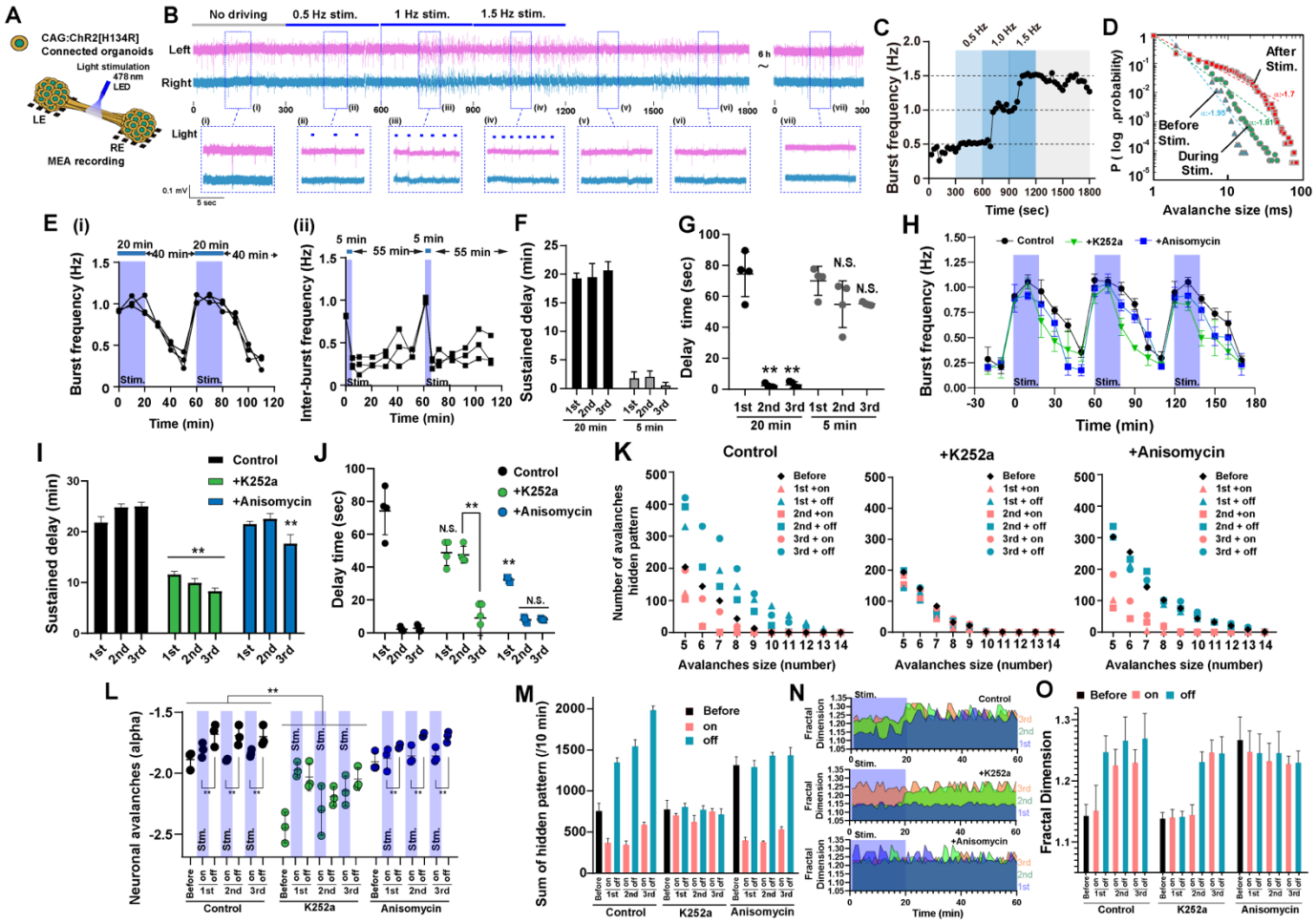

Fig. 4. Short-term memory in the connected organoids

(A) Optogenetic simulation of the axonal bundle with a 470 nm laser drove synchronized burst activity at 0.5, 1, and 1.5 Hz frequency. The effect of stimulation persisted after cessation of illumination but did not for 6 hours. (B, C) Burst frequency modulated by the optical stimulation. The burst frequency followed the stimulation frequency after a significant time lag. (D) Log plot of neuronal avalanche size and probability before, during, and after the stimulation. (E) Time-course of burst frequency with 1 Hz stimulation for 20 min (i) or 5 min (ii) every 1 hour. (F) Duration until the burst frequency decreased to 75% of the maximum burst frequency after cessation of light stimulation. (G) Time lag from the start of light stimulation to induction of burst frequency was significantly reduced during the second and third attempt compared to that during the first attempt when the connected organoids were stimulated for 20 min. (H) Time series of burst frequency in the presence of K252a or anisomycin. (I) Duration of sustained activity of the connected organoids during treatment with the compounds. (J) Delay time in the presence of K252a and anisomycin. (K) Hidden patterns in neuronal avalanches were altered by the drug treatment. (L) Probability slope of neuronal avalanches. K252a treatment, but not anisomycin treatment, led to a decreased probability of neuronal avalanches. (M) Less hidden patterns were observed during the light-on than during the light-off period. K252a treatment suppressed the number of hidden patterns even after repeated training. (N, O) Fractal dimensions of LFP signal. Fractal dimensions increased after cessation of light stimulation during the first attempt in the

control condition and during the second attempt in the K252a-treated condition. *$p<0.05$, **$p<0.01$; one-way ANOVA. Error bars indicate SD.

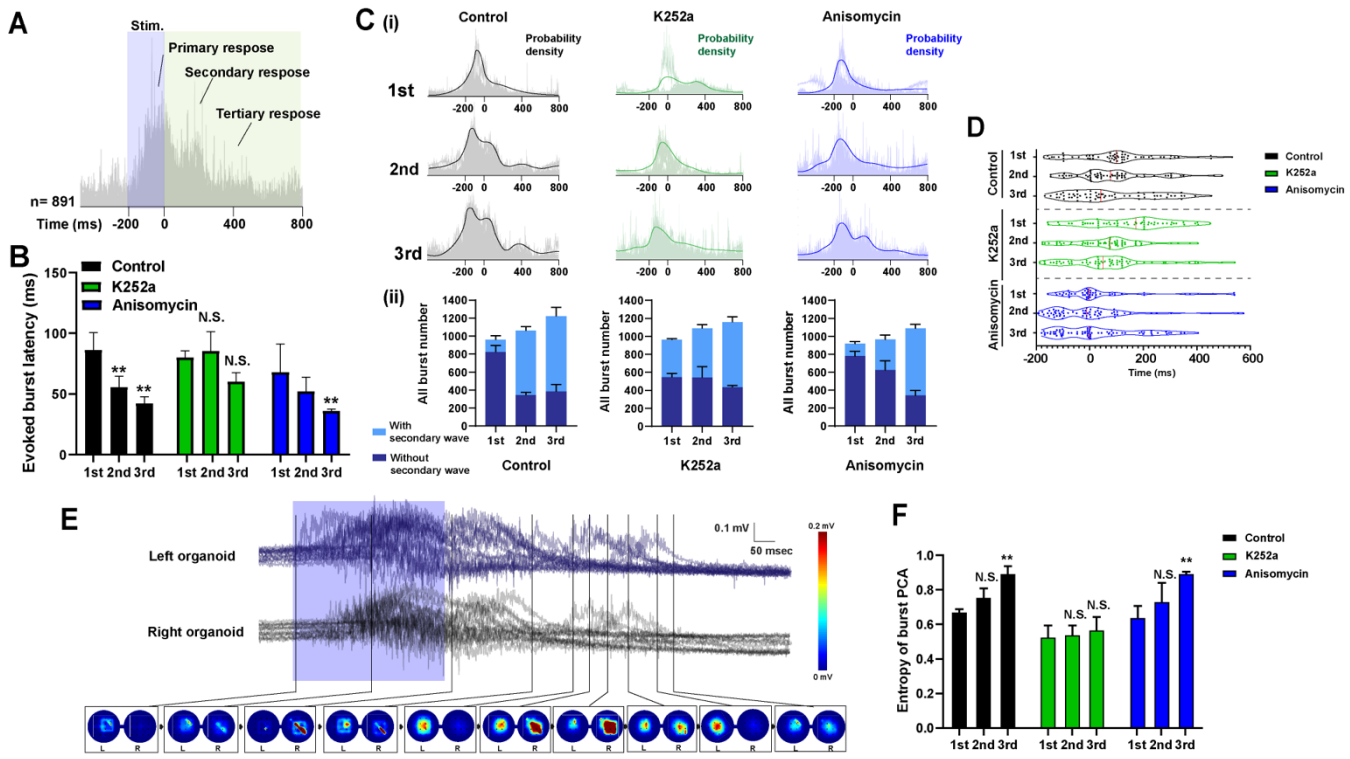

Fig. 5. Diverse evoked burst patterns supported by CaMKII-dependent signaling

(A) Representative image of sorted evoked bursts by optogenetic stimulation and color-coded map depicting the voltage distribution from neurons in left and right cerebral organoids. A total of 891 burst traces is presented. Light stimulation induced evoked spikes, and the burst waves persisted after light stimulation. Secondary, and tertiary waves were also observed. (B) Latency of the evoked bursts. Repeated light stimulation (at second and third attempts) significantly decreased evoked burst latency in control and anisomycin-treated conditions, whereas K252a treatment did not influence the latency of evoked bursts. n = 3. (C) (i) Overlayed power histograms of evoked bursts and kernel density estimation (line) in the presence of K252a and anisomycin. Repeated light stimulation increased burst wave complexity. (ii) Percentage of evoked bursts with and without secondary peaks. (D)Violin plots of burst wave peak times. n = 50. (E) Representative crosstalk between the two connected organoids in self-evoked bursts. (F) Quantification of the diversity by calculating entropy of burst PCA. n = 3. *p<0.05, **p<0.01; one-way ANOVA or student's t-test. Error bars indicate SD.